



Climatology of the ionospheric slab thickness along the longitude of 120° E in China and its adjacent region during the solar minimum years of 2007–2009

Z. Huang¹ and H. Yuan²

¹School of Physics and Electronic Engineering, Jiangsu Normal University, Xuzhou, 221116, China

²Academy of Opto-Electronics, the Chinese Academy of Sciences, Beijing, 100094, China

Correspondence to: Z. Huang (wang86516@163.com)

Received: 3 June 2015 – Revised: 14 September 2015 – Accepted: 9 October 2015 – Published: 30 October 2015

Abstract. The ionospheric slab thickness is defined as the ratio of the total electron content (TEC) to the ionospheric F2 layer peak electron density ($NmF2$). In this study, the slab thickness is determined by measuring the ionospheric TEC from dual-frequency Global Positioning System (GPS) data and the $NmF2$ from the Constellation Observing System for Meteorology, Ionosphere and Climate (COSMIC). A statistical analysis of the diurnal, seasonal and spatial variation in the ionospheric slab thickness is presented along the longitude of 120° E in China and its adjacent region during the recent solar minimum phase (2007–2009). The diurnal ratio, defined as the maximum slab thickness to the minimum slab thickness, and the night-to-day ratio, defined as the slab thickness during daytime to the slab thickness during night-time, are both analysed. The results show that the TEC of the northern crest is greater in winter than in summer, whereas $NmF2$ is greater in summer than in winter. A pronounced peak of slab thickness occurs during the post-midnight (00:00–04:00 LT) period, when the peak electron density is at the lowest level. A large diurnal ratio exists at the equatorial ionization anomaly, and a large night-to-day ratio occurs near the equatorial latitudes and mid- to high latitudes. It is found that the behaviours of the slab thickness and the F2 peak altitude are well correlated at the latitudes of 30–50° N and during the period of 10:00–16:00 LT. This current study is useful for improvement of the regional model and accurate calculation of the signal delay of radio waves propagating through the ionosphere.

Keywords. Ionosphere (equatorial ionosphere)

1 Introduction

The ionospheric total electron content (TEC) represents the number of free electrons in a cross-section column along the ray path from a receiver to a satellite. It is one of the most important parameters for characterizing ionosphere properties. With increasing demands on trans-ionospheric communication systems, the actual TEC values are becoming more and more important for appropriate ionospheric refraction corrections. Since the Global Positioning System (GPS) was put into service, it has become an effective technique for the continuous measurement of TEC in different geographic locations. The peak electron density of the F2 layer ($NmF2$), which is closely related to TEC, is primarily used to describe the features of the ionospheric F2 region.

The ionospheric slab thickness (τ) can be defined as the ratio of vertical TEC (VTEC) to the electron density at the peak of the F2 layer ($NmF2$):

$$\tau = \text{VTEC}/NmF2, \quad (1)$$

where the vertical TEC is given in TEC units (electrons per square metre), $NmF2$ is in electrons per cubic metre, and τ is in metres. Slab thickness is an important parameter of a hypothetical ionosphere that has the same TEC as the actual ionosphere and constant uniform density equal to that of the F2 peak (Chuo, 2007). It is capable of offering substantial information on many ionospheric phenomena and processes (Jayachandran et al., 2004) and is therefore employed in modelling the ionosphere, such as the International Reference Ionosphere (IRI) (Bilitza, 2001).

Ionospheric slab thickness has been a subject of study since the 1960s (e.g. Bhonsle et al., 1965; Titheridge, 1973;

Huang, 1983). Based on most of the available and reliable observations of ionospheric TEC and $NmF2$, numerous analyses for recording the climatology of the slab thickness have been conducted over the past few decades (Jayachandran et al., 2004; Chuo, 2007; Jin et al., 2007; Stankov and Warnant, 2009; Guo et al., 2011; Kenpankho et al., 2011; Weng et al., 2012). Jayachandran et al. (2004) investigated the variation in the slab thickness during the solar maximum and minimum phases of an intense solar cycle by using the hourly values of TEC and $NmF2$ at Hawaii (low latitude), Boulder (mid-latitude) and Goosebay (high latitude). It was revealed that the slab thickness varies with diurnal, seasonal, geomagnetic and solar activity. Stankov and Warnant (2009) described the climatological and storm-time behaviour of the slab thickness based on long-term observations at a European mid-latitude site (Dourbes), which further confirmed the expected diurnal, seasonal, and geomagnetic dependency. Guo et al. (2011) reported the latitudinal variation in the slab thickness using global ionospheric maps (GIMs) and the Constellation Observing System for Meteorology, Ionosphere and Climate (COSMIC). Moreover, all above-mentioned studies have indicated that the diurnal, seasonal, solar and geomagnetic activity variations in the slab thickness significantly depend on the location of the observing station.

A constellation of six microsatellites, termed COSMIC (also known as FORMOSAT-3 in Taiwan), was launched on 15 April 2006 (Kumar, 2006). Each COSMIC satellite houses a GPS Occultation Experiment (GOX) payload to operate the radio occultation measurement, and it now provides a new data source for understanding global ionospheric structures and behaviours. Globally, an average of approximately 1800 electron density profiles can be provided in a day. Electron density profiles can be retrieved from delay measurements of GPS signals received by low Earth orbit (LEO) satellites by using the Abel inversion technique under the assumption of local spherical symmetry of the ionosphere (Schreiner, 1999). However, the local spherical symmetry may be a strong assumption, and the horizontal structure may affect the retrieved density profiles in some cases. The quality of COSMIC occultation measurements was validated by comparing the data of incoherent scatter radar with those of ionosondes (Lei et al., 2007; Kelley et al., 2009; Sun et al., 2014), which revealed good agreement. Liu et al. (2010) and Yue et al. (2010) showed that the Abel retrieval provided an accurate ionospheric $NmF2$ and F2 layer peak height ($HmF2$) from radio occultation measurements. Hence, COSMIC is a powerful system for global or regional mapping of the ionospheric $NmF2$ and slab thickness because of its global coverage and high vertical resolution.

The objectives of the present paper are to verify the characteristic features of temporal, seasonal and spatial variations in slab thickness measured by the COSMIC ionospheric radio occultation (IRO) along the longitude of 120° E in China and its adjacent region during the low-solar-activity period

of 2007–2009. The study provides a better understanding of the morphology and possible mechanisms of the peak of slab thickness in China sector, and it also benefits the development of regional ionosphere modelling and the estimation of the ionospheric delay correction. The paper is organized as follows: in Sect. 2, a GIM-aided method is described for estimating vertical ionospheric TEC. In Sect. 3, the climatology of the ionospheric parameters is analysed, with an emphasis on the diurnal, latitudinal and seasonal variations in slab thickness. A discussion and our conclusions are given in Sects. 4 and 5, respectively.

2 A method for estimating the ionospheric vertical TEC

Dual-frequency carrier-phase and code-delay GPS observations are combined to obtain slant ionospheric TEC along the satellite–receiver line of sight. However, the measured slant TEC includes differential code biases (DCBs) due to the transmitting and receiving hardware and can be expressed as

$$STEC' = STEC + bs + br, \quad (2)$$

where $STEC'$ is the measured slant TEC and $STEC$ is the actual slant TEC, and bs and br are the satellite and receiver bias, respectively. The vertical TEC is computed from

$$VTEC = STEC \cdot \sin(E_i) = STEC \cdot \sqrt{1 - \left(\frac{R_e \cos(E_0)}{R_e + h_m}\right)^2}, \quad (3)$$

where $VTEC$ is the actual vertical TEC and E_i is the elevation angle at the ionospheric pierce point (IPP), known as the intersect point of the satellite–receiver line of sight passing through the ionospheric thin shell at a flexible altitude (h_m). R_e is the mean radius of the Earth, and E_0 is the elevation angle at the receiver location.

Most techniques estimate the actual vertical ionospheric structure, and simultaneously the GPS systemic biases are treated as nuisance parameters over periods of 24 h or even longer. Through use of a Kalman filter or sequential least-squares method, these biases can be removed from the slant TEC measurements; thus an unbiased vertical TEC is obtained (Sardon et al., 1994; Huang et al., 2003). However, large errors are introduced in the estimation of the vertical TEC for the low-latitude region (Rama Rao et al., 2006; Huang and Yuan, 2013). In this study, to minimize the error, we utilize the products provided by the Center for Orbit Determination in Europe (CODE) to estimate the DCBs. At first, the GPS satellite DCB is calibrated using the CODE results, which are obtained by using the least-squares fitting based on global observations. Then, the DCB of GPS receiver is estimated by using the method proposed by Komjathy et al. (2005). For each slant TEC of a receiver, its vertical TEC at the IPP is assumed to be equal to the corresponding vertical TEC from the CODE GIMs. The difference be-

Table 1. The locations of the GPS stations.

Stations	Latitude (° N)	Longitude (° E)
PIMO	14.64	121.08
TCMS	24.8	120.99
WUHN	30.53	114.36
SHAO	31.10	121.20
DAEJ	36.40	127.37
BJFS	39.61	115.89
CHAN	43.79	125.44
YAKE	62.03	129.68

tween two vertical TEC values is treated as the specific receiver DCB. Many DCBs for each receiver are collected during a day and then a daily average of DCBs is obtained for the specific receiver. It should be noted that the ionospheric thin shell is fixed at an altitude of 450 km, which is the same as that of the CODE GIM construction. The method can provide accurate estimations of DCB and vertical TEC. To minimize unwanted errors, the cutoff elevation angle of 20° is used for each GPS receiver.

3 Data and results

From the above algorithm, the vertical TEC distribution with interval of 30 s is obtained from the ground stations at different latitudes along the longitude of 120° E. The locations of the GPS stations are listed in Table 1.

The diurnal and seasonal variations in ionospheric parameters are investigated for the low-solar-activity period of 2007–2009. The 10.7 cm solar radio radiation flux (F107) is shown in Fig. 1. As can be seen in this figure, all of the F107 indices are below 100 SFU (SFU: solar flux unit; 1 SFU = 10⁻²² W m⁻² Hz⁻¹) and the mean F107 value is approximately 70 SFU in the years of 2007–2009. Compared to the extreme solar minimum in 2008/2009, the solar activity in 2007 is higher. Here, the 90-day windows centred at the March equinox, June solstice, September equinox and December solstice are denoted as spring, summer, autumn and winter, respectively.

To avoid the negative effect of poor-quality data from COSMIC RO measurements, the noise level factor (δ) of an occultation event is defined as (Guo et al., 2011)

$$\delta = \sqrt{\frac{\sum_{i=1}^k (n_e(i) - \bar{n}_e(i))^2}{k(NmF2)^2}}, \quad (4)$$

where $n_e(i)$ is the electron density profile above 300 km, $\bar{n}_e(i)$ is the smooth density profile, and k is the total number of the data. The poor-quality data with a large level of noise (>0.01) are removed in this study.

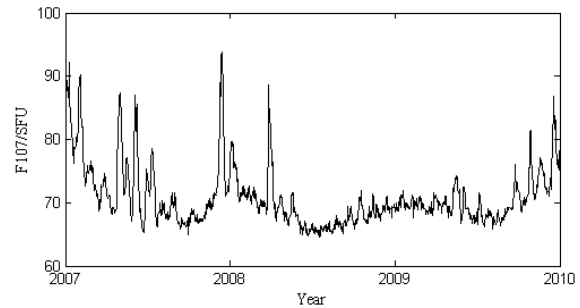


Figure 1. F107 variations during the solar minimum of 2007–2009.

The TEC from ground-based GPS measurements and the $NmF2$ from COSMIC RO measurements provided by CDAAC are binned in a uniform grid with a resolution of 5° N latitude and 2 h in local time. For each subset, a discretized smoothing spline technique proposed by Garcia (2010) is applied to address occurrences of missing and outlying data. The technique, based on a penalized least-squares method, allows for the amount of smoothing to be automatically chosen by minimizing the generalized cross-validation score, and it provides an efficient smoother for numerous applications in the area of data analysis. The contour maps in Fig. 2 illustrate the latitudinal and diurnal variations in TEC in all seasons during the period of 2007–2009. The data in the figure represent the median TEC in the bin of 2 h and 5°. As shown in the figure, the peak values of TEC occur between 12:00 and 18:00 LT, and the minimum values occur between 00:00 and 04:00 LT. The equatorial ionization anomaly (EIA; the daytime equatorial and low-latitude ionosphere is characterized by an electron density trough at the geomagnetic equator and two crests within ± 10 – 30° magnetic latitude) is clearly observed in all seasons. Strong seasonal variations in TEC are found to be maximum in the spring and minimum in the summer in both 2008 and 2009. An obvious winter anomaly exists, with the magnitude of peak TEC in the winter higher than that in summer. The TEC peak in 2007 is larger compared to other years, which might be attributed to the higher solar activity in 2007. Figure 3 shows the latitudinal and diurnal variation in $NmF2$ derived from COSMIC measurements in all seasons. The diurnal variation in $NmF2$ pattern follows a similar trend to the TEC variation shown in Fig. 2. However, the minimum $NmF2$ values occur in winter, and the winter anomaly is not clear from 2007 to 2009.

The slab thickness is directly calculated using Eq. (1), and the associated diurnal, latitudinal and seasonal variations are presented in Fig. 4. It is obvious that the variations in slab thickness with the night-time values (00:00–04:00 LT) are substantially higher than the day-time values (08:00–18:00 LT) in all seasons. The slab thickness peak at night mainly occurs in mid- to low latitudes during the study period of 2007–2009. During night-time, the maximum peak of slab thickness in summer and winter is comparatively higher than

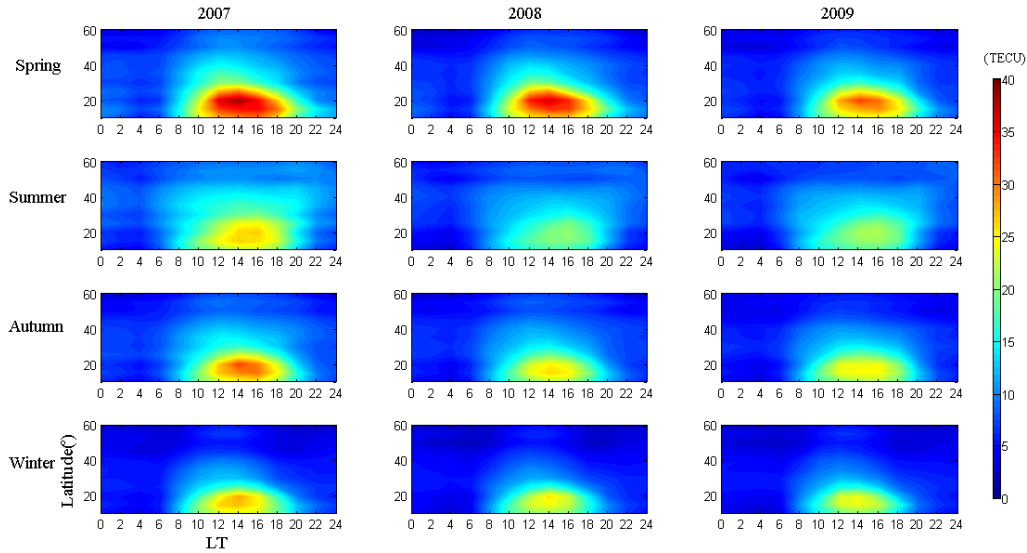


Figure 2. Latitudinal, diurnal and seasonal variation in TEC during the low-solar-activity period of 2007–2009.

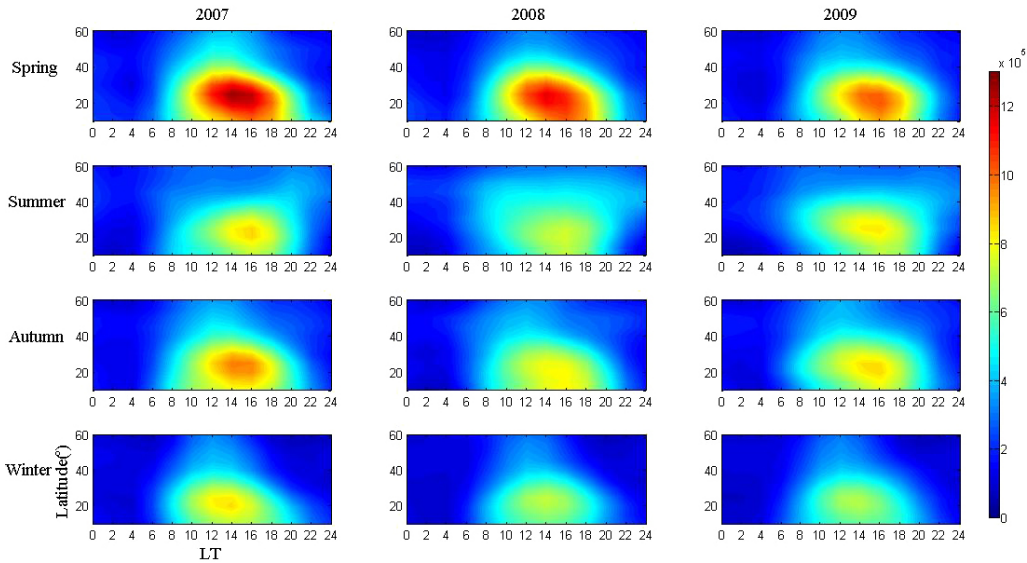


Figure 3. Latitudinal, diurnal and seasonal variation in *NmF2* during the low-solar-activity period of 2007–2009.

that in spring and autumn. In addition, the post-sunset enhancement can be observed at mid- to high latitudes in most cases, particularly in winter. In the mid-afternoon, the variation in slab thickness in the near-equatorial region is higher than that observed in other regions, whose values are approximately 400 km.

In order to further explore the latitudinal variation in the slab thickness in all seasons, the diurnal ratio, which is defined as the maximum slab thickness to the minimum slab thickness per day, is analysed. Further, the night-to-day ratio is defined as the slab thickness during the daytime (08:00–16:00 LT) to the slab thickness during the night-time (22:00–04:00 LT). The diurnal ratio and the median night-to-day ra-

tios are shown in the upper and lower panels of Fig. 5. The figure shows that the diurnal ratios at latitudes 25–35° N located in the northern crest equatorial anomaly are the highest in winter during the low solar activity of 2007–2009, and the ratio reaches a value of approximately 3.8 in some cases. The night-to-day ratios of the equatorial region are the most pronounced, and the ratios in the mid- to high latitudes are comparatively large, particularly in summer. It is determined that, for the diurnal ratios, the night-to-day ratios in the northern crest equatorial anomaly are smaller in winter but larger in summer. The difference between the types of ratios is the most significant under conditions of peak slab thickness referring to the sunrise/sunset hours, when the ionosphere–

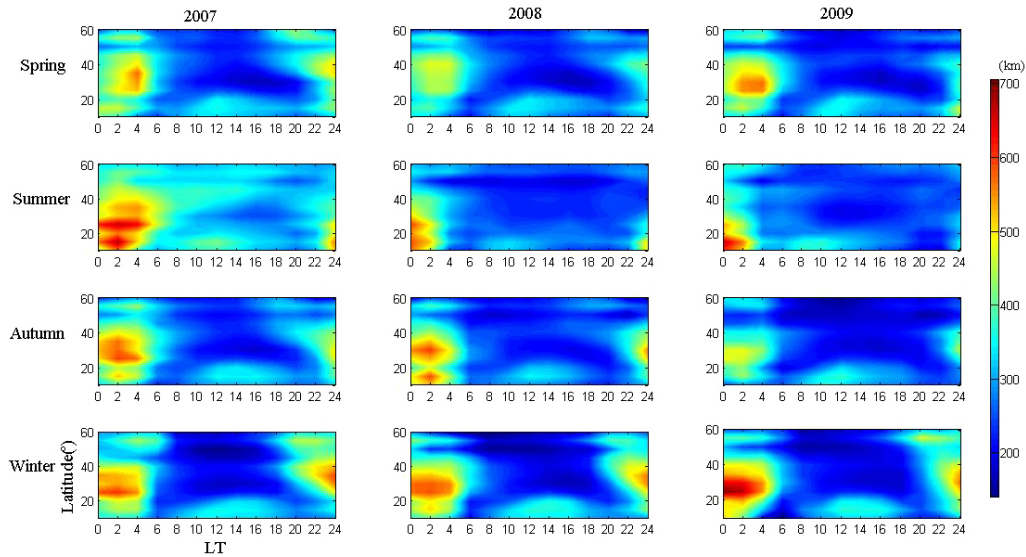


Figure 4. Latitudinal, diurnal and seasonal variation in slab thickness during the low-solar-activity period of 2007–2009.

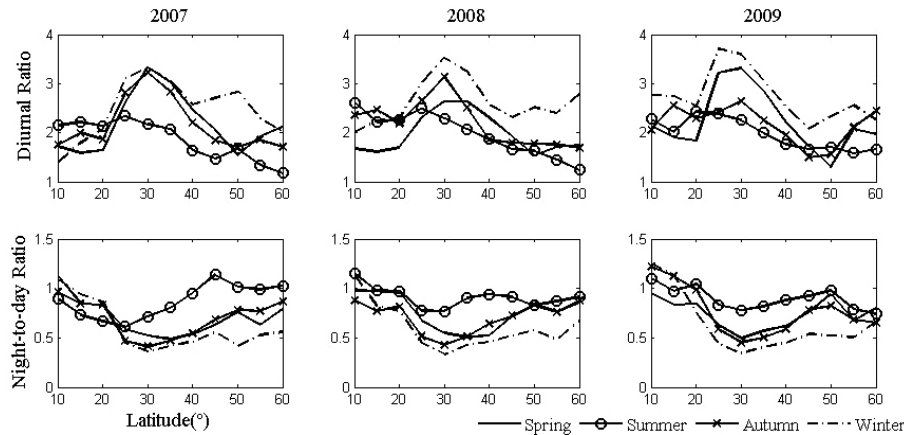


Figure 5. Latitudinal and seasonal variation in the diurnal ratio and the median night-to-day ratio for the years of 2007–2009.

protonosphere plasma flux changes direction (Jayachandran et al., 2004).

HmF2 is also one of the most important parameters; the latitudinal and diurnal variations in *HmF2* are analysed and the results of this are shown in Fig. 6. As illustrated in Fig. 6, the *HmF2* in the low latitudes is generally large during the period of 10:00–16:00 LT. Additionally, the *HmF2* peak is clearly observed from post-sunset to post-midnight (00:00–04:00 LT); it shows a similar trend to the variation in the slab thickness during the same period in some cases. The correlation analysis between the slab thickness and the F2 layer peak altitude is further performed during the solar minimum of 2007–2009. The latitudinal correlation coefficient and the temporal correlation coefficient are analysed and the results are shown in Fig. 7. It can be seen from the upper panels in Fig. 7 that the slab thickness and the F2 layer peak altitude in mid-latitudes (30–50° N) exhibit a strong correlation. How-

ever, the correlation is relatively weak in the low latitudes (10–25° N) and at high latitude (60° N). From the lower panels, the behaviours of the slab thickness and the F2 peak altitude are well correlated in the daytime but show weak correlation during post-midnight in most cases. The correlation decreases to almost 0 or even lower at around sunrise and post-sunset.

4 Discussion

In this work, the TEC winter anomaly at low latitude is clearly observed, while *NmF2* is not. COSMIC *NmF2* shows strong annual asymmetry during the solar minimum (2007–2009), with smaller values near the June solstice than near the December solstice (Qian et al., 2013; Xue et al., 2015). The *NmF2* variation is not consistent with our result, which

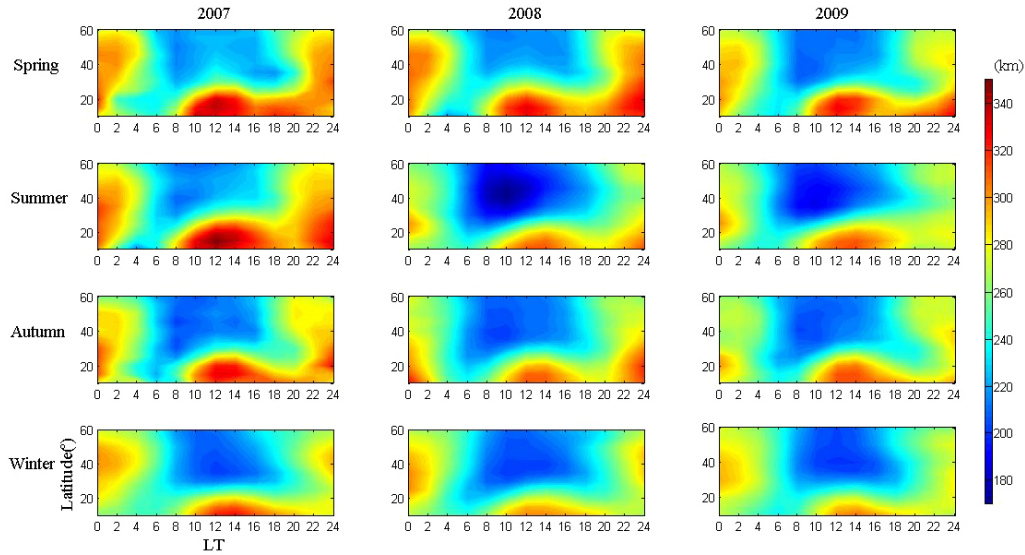


Figure 6. Latitudinal, diurnal and seasonal variation in *HmF2* during the low-solar-activity period of 2007–2009.

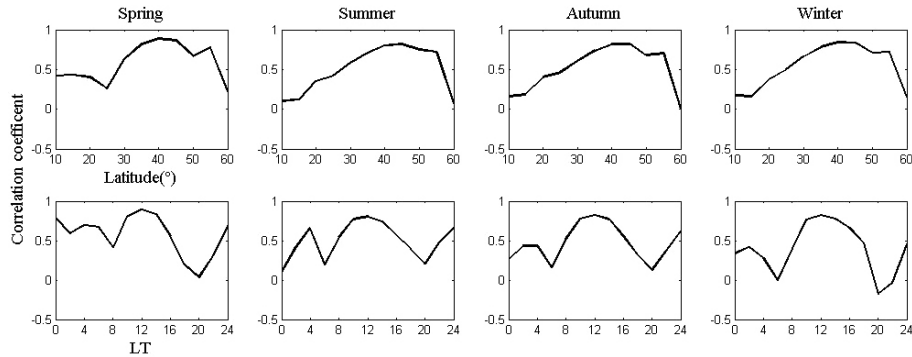


Figure 7. Correlation coefficient between the slab thickness and the F2 layer peak altitude for geographic latitude (top panels) and local time (bottom panels) in all seasons during the solar minimum.

is probably due to the spatial and temporal coverage of data. The data collected by Qian et al. (2013) and Yue et al. (2015) cover the globe for all longitudes, while our data source is in China and its adjacent region at the longitude of 120° E. Additionally, a 30-day running median is applied for a global monthly map of *NmF2* in their studies, while a 90-day interval centred at the equinox/solstice is processed with a smoothing technique for a regional seasonal map in this study.

The height of the GPS orbit is 20 200 km above Earth’s surface, and most parts of the propagation path of a radio signal are within the plasmasphere from a satellite to a ground-based receiver. Hence, GPS TEC can be considered the combined contribution of the ionosphere and the overlying plasmasphere. The international standard plasmasphere–ionosphere model (SPIM) (Gulyaeva and Bilitza, 2012; Gulyaeva et al., 2013) combines the International Reference Ionosphere (IRI) with the Russian standard model of

the ionosphere and plasmasphere (SMI). One of the advantages of this model is that it can provide TEC at altitudes of 80 to 35 000 km for any location on Earth. In this work, for a given geographic location (latitude and longitude) and local time, we employed SPIM to obtain TEC estimates (100–20 000 km) along 120° E in 2008 and then compared it with the GPS TEC. It is found that the modelled median TEC is overestimated but is closely correlated with the GPS TEC. By comparison, COSMIC observations and SPIM simulations exhibit good agreement in the estimation of bottom-side TEC, topside TEC and plasmaspheric TEC (Zakharenkova et al., 2012). Hence, distributions of TEC are analysed for bottom-side (100–*HmF2*), topside (*HmF2*–1336 km) and plasmaspheric TEC (1336–20 000 km), and results of this are shown in Fig. 8. The distributions of TEC indicate that the topside ionosphere and plasmasphere exhibit the TEC winter anomaly feature, whereas the bottom side does not.

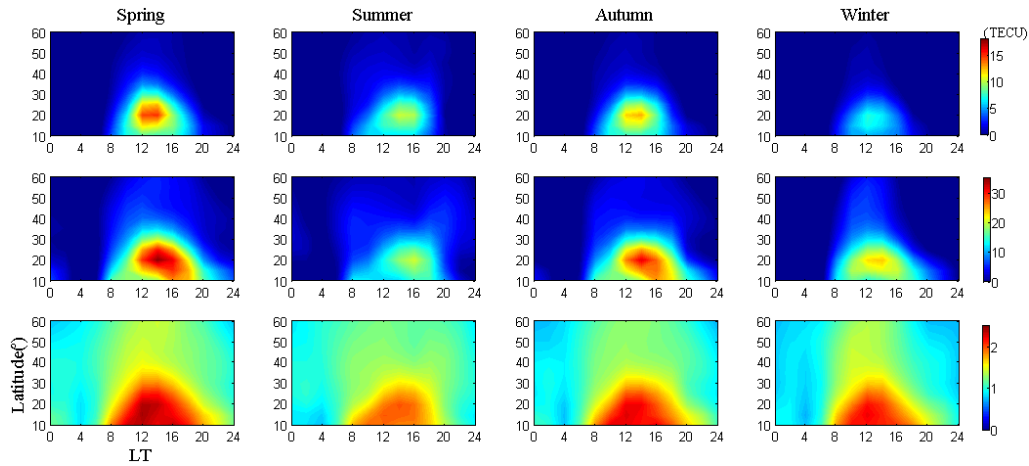


Figure 8. Two-dimensional distribution of bottom-side TEC (top panels), topside TEC (middle panels) and plasmaspheric TEC (bottom panels) in 2008.

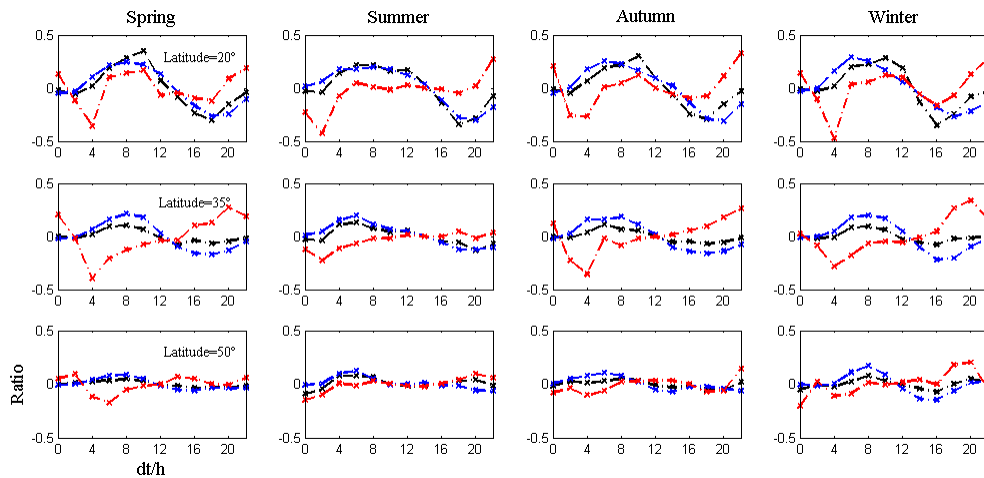


Figure 9. Ratio variation in TEC (black broken line), $NmF2$ (blue broken line) and slab thickness (red broken line) for all seasons in 2008.

The winter anomaly was explained using the change in composition of the atmosphere, especially in the ratio of the concentrations of atomic oxygen and molecular nitrogen (e.g. Rishbeth and Setty, 1961; Rüster and King, 1973; Yu et al., 2004). The changes in composition were influenced by the vertical and horizontal neutral winds associated with a worldwide thermospheric circulation, and the atomic/molecular ratio in winter is higher than in summer by summer-to-winter transport. However, we can not clearly observe the winter anomaly of $NmF2$. The winter anomaly can not be simply attributed to the ratio of $[O/N_2]$. Another possible mechanism of the direction change of neutral wind that results from the coupling of the neutral gas and plasma (Su et al., 1998) may have a significant contribution.

It can be easily determined that the variation in ionospheric slab thickness with local time depends on the variation in TEC and $NmF2$ obtained from Eq. (1). To better understand the possible formation mechanisms of the peak of slab thick-

ness, the ratio κ is defined as the temporal variation in the ionospheric parameters (TEC, $NmF2$ and τ):

$$\kappa = d\lambda/dt . \tag{5}$$

In this work, the data from 2008 are taken as an example. First, the ionospheric parameters are normalized, and then their temporal ratios at different latitudes are analysed according to Eq. (5). The ratio variations in TEC, $NmF2$ and slab thickness at latitudes of 20° N (top panels), 35° N (middle panels) and 55° N (bottom panels), respectively, are shown in Fig. 9. The ratio variations in TEC and $NmF2$ show a similar trend: they increase before mid-afternoon, then decrease, and then increase again around sunset. The significant decrease in the ratio variation in slab thickness before sunrise can be observed at the latitudes of 20 and 35° N; the minimum value is approximately -0.4 . However, the temporal ratio variation is relatively smooth at a latitude of 50° N. The increase in TEC and $NmF2$ results in decreased slab

thickness because the increase in TEC is slower than that of $NmF2$. From around sunset to midnight, the temporal ratio of TEC is higher than that of $NmF2$, which leads to an enhancement in slab thickness. A pronounced peak of slab thickness at night at low and mid-latitudes was reported during the solar minimum in some early studies, and a number of theories have been put forward to explain this phenomenon (Titheridge, 1973; Rastogi, 1988; Davies and Liu, 1991). Davies and Liu (1991) have suggested that the pre-sunrise peak in the slab thickness is related to the maintenance of the night-time F layer, and it was well explained by the lowering of the ionospheric F layer immediately before sunrise to regions of greater neutral density, leading to increased ion loss due to dissociative recombination. However, some scientists have suggested that the phenomenon may also be associated with the night-time enhancements in TEC, which are mainly due to the field-aligned plasma flow from the protonosphere to the ionosphere (Minakoshi and Nishimuta, 1994). In this work, a TEC temporal ratio less than 0 indicates that the explanation related to chemical combination is reasonable for the study region.

Compared with previous work (Guo et al., 2011), the occurrence of the peaks of slab thickness in this study is later; this may result from the difference in spatial coverage of data. The slab thickness in Guo et al. (2011) work was calculated by using the median $NmF2$ from all longitudes, while ours is calculated through the $NmF2$ at the longitude of 120° E described above. Moreover, the TEC measurements used by Guo et al. (2011) were derived from geographical and time interpolations of the global ionospheric map provided by CODE, but the TEC measurements in this work are from dual-frequency GPS. Both data processing and resources may contribute to the discrepancy in the slab thickness variation.

5 Conclusions

The climatology of ionospheric TEC, $NmF2$ and equivalent slab thickness is analysed by using dual-frequency ground-based GPS observations and COSMIC IRO measurements along the longitude of 120° E in China and its adjacent region during the solar minimum years of 2007–2009. The correlation of slab thickness with $HmF2$ is discussed and the following results are obtained:

1. Strong seasonal variation and EIA in TEC are observed. Ionospheric $NmF2$ follows a similar trend to TEC variation, but the winter anomaly is not observed in $NmF2$.
2. The maximum value of slab thickness is approximately 700 km at night in the low and mid-latitudes when the peak electron density is at a low level. During the daytime, the maximum slab thickness in the equatorial latitudes is approximately 400 km. The occurrence of the

post-sunset enhanced slab thickness is obvious in winter in the mid- to high latitudes (30–60° N).

3. The diurnal ratios of slab thickness vary from 1.2 to 4, with the maximum value occurring in the EIA crest in winter. The night-to-day ratios of slab thickness vary from 0.4 to 1.2, with the large values occurring near the equatorial and mid- to high latitudes.
4. Slab thickness shows a strong correlation with $HmF2$ at mid- to high latitudes and a weak correlation at low latitudes.

Acknowledgements. Dual-frequency GPS and COSMIC IRO data were provided by the International GNSS Service and the COSMIC Data Analysis and Archive Center (CDAAC). This research was supported by the National Natural Science Foundation of China (41104096).

The topical editor H. Kil thanks S. Stankov and one anonymous referee for help in evaluating this paper.

References

- Bhonsle, R. V., Da Rosa, A. V., and Garriott, O. K.: Measurement of total electron content and equivalent slab thickness of the mid-latitude ionosphere, *Radio Sci.*, 69, 929–939, 1965.
- Bilitza, D.: International reference ionosphere 2000, *Radio Sci.*, 36, 261–275, 2001.
- Chuo, Y. J.: The variation of ionospheric slab thickness over equatorial ionization area crest region, *J. Atmos. Sol.-Terr. Phys.*, 69, 947–954, 2007.
- Davies, K. and Liu, X. M.: Ionospheric slab thickness in middle and low-latitudes, *Radio Sci.*, 26, 997–1005, 1991.
- Garcia, D.: Robust smoothing of gridded data in one and higher dimensions with missing values. *Computational statistics & data analysis*, 54, 1167–1178, 2010.
- Gulyaeva, T. L. and Bilitza, D.: Towards ISO standard earth ionosphere and plasmasphere model, *New developments in the standard model*, Nova Science Publishers, Hauppauge, New York, USA, 1–39, 2012.
- Gulyaeva, T. L., Arikani, F., Hernandez-Pajares, M., and Stanislawska, I.: GIM-TEC adaptive ionospheric weather assessment and forecast system. *J. Atmos. Sol.-Terr. Phys.*, 102, 329–340, doi:10.1016/j.jastp.2013.06.011, 2013.
- Guo, P., Xu, X., and Zhang, G. X.: Analysis of the ionospheric equivalent slab thickness based on ground-based GPS/TEC and GPS/COSMIC RO measurements, *J. Atmos. Sol.-Terr. Phys.*, 73, 839–846, 2011.
- Huang, Y. N.: Some result of ionospheric slab thickness observations at Luning, *J. Geophys. Res.*, 88, 5517–5522, 1983.
- Huang, Z., Yuan, H., and Wan, W. X.: Test of GPS TEC hardware biases estimating methods, *Chinese Journal of Radio Science*, 18, 472–476, 2003.
- Huang, Z. and Yuan, H.: Analysis and improvement of ionospheric thin shell model used in SBAS for China region, *Adv. Space Res.* 51, 2035–2042, 2013.

- Jayachandran, B., Krishnankutty, T. N., and Gulyaeva, T. L.: Climatology of ionospheric slab thickness, *Ann. Geophys.*, 22, 25–33, doi:10.5194/angeo-22-25-2004, 2004.
- Jin, S. G., Cho, J. H., and Park, J. U.: Ionospheric slab thickness and its seasonal variations observed by GPS, *J. Atmos. Terr. Phys.*, 69, 1864–1870, 2007.
- Kelley, M. C., Wong, V. K., Aponte N., Coker, C., Mannucci, A. J., and Komjathy, A.: Comparison of COSMIC occultation-based electron density profiles and TIP observations with Arecibo incoherent scatter radar data, *Radio Sci.*, 44, RS4011, doi:10.1029/2008RS004087, 2009.
- Kenpankho, P., Supnithi, P., Tsugawa, T., and Maruyama, T.: Variation of ionospheric slab thickness observations at Chumphon equatorial magnetic location, *Earth Planets Space*, 63, 359–364, 2011.
- Komjathy, A., Sparks, L., Wilson, B. D., and Mannucci, A. J.: Automated daily processing of more than 1000 ground-based GPS receivers for studying intense ionospheric storms, *Radio Sci.*, 40, RS6006, doi:10.1029/2005RS003279, 2005.
- Kumar, M.: New satellite constellation uses radio occultation to monitor space weather, *Space Weather*, 4, S05003, doi:10.1029/2006SW000247, 2006.
- Lei, J. H., Syndergaard, S., Burns, A. G., Solomon, S. C., Wang, W. B., Zeng, Z., Roble, R. G., Wu, Q., Kuo, Y. H., Holt, J. M., Zhang, S. R., Hysell, D. L., Rodrigues, F. S., and Lin, C. H.: Comparison of COSMIC ionospheric measurements with ground-based observations and model predictions: Preliminary results, *J. Geophys. Res.*, 112, A07308, doi:10.1029/2006JA012240, 2007.
- Liu, J. Y., Lin, C. Y., Lin, C. H., Tsai, H. F., Solomon, S. C., Sun, Y. Y., Lee, I. T., Schreiner, W. S., and Kuo, Y. H.: Artificial plasma cave in the low-latitude ionosphere results from the radio occultation inversion of the FORMOSAT-3/COSMIC, *J. Geophys. Res.*, 115, A07319, doi:10.1029/2009JA015079, 2010.
- Minakoshi, H. and Nishimuta, I.: Ionospheric electron content and equivalent slab thickness at lower mid-latitudes in the Japanese zone, *Proc. IBSS, University of Wales, UK*, 144 pp., 1994.
- Qian, L., Burns, A. G., Solomon, S. C., and Wang, W.: Annual/semiannual variation of the ionosphere, *Geophys. Res. Lett.*, 40, 1928–1933, 2013.
- Rama Rao, P. V. S., Niranjana, K., Prasad, D. S. V. V. D., Gopi Krishna, S., and Uma, G.: On the validity of the ionospheric pierce point (IPP) altitude of 350 km in the Indian equatorial and low-latitude sector, *Ann. Geophys.*, 24, 2159–2168, doi:10.5194/angeo-24-2159-2006, 2006.
- Rastogi, R. G.: Collapse of the equatorial ionosphere during the sunrise period, *Ann. Geophys.*, 6, 205–209, 1988, <http://www.ann-geophys.net/6/205/1988/>.
- Rishbeth, H. and Setty, C.: The F layer at sunrise, *J. Atmos. Terr. Phys.*, 20, 263–267, 1961.
- Rüster, R. and King, J. W.: Atmospheric composition changes and the F2-layer seasonal anomaly, *J. Atmos. Terr. Phys.*, 35, 1317–1322, 1973.
- Sardon, E., Rius, A., and Zarraoa, N.: Estimation of transmitter and receiver differential biases and the ionospheric total electron content from global positioning system observations, *Radio Sci.*, 29, 577–586, 1994.
- Schreiner, W. S., Sokolovskiy, S. V., Rocken, C., and Hunt, D. C.: Analysis and validation of GPS/MET radio occultation data in the ionosphere, *Radio Sci.*, 34, 949–966, 1999.
- Stankov, S. M. and Warnant, R.: Ionospheric slab thickness-analysis, modelling, and monitoring, *Adv. Space Res.*, 44, 1295–1303, 2009.
- Su, Y. Z., Bailey, G. J., and Oyama, K.-I.: Annual and seasonal variations in the low-latitude topside ionosphere, *Ann. Geophys.*, 16, 974–985, doi:10.1007/s00585-998-0974-0, 1998.
- Sun, L. F., Zhao, B. Q., Yue, X. A., and Mao, T.: Comparison between ionospheric character parameters retrieved from FORMOSAT3 measurement and ionosonde observation over China, *Chinese J. Geophys.*, 57, 3625–3632, doi:10.6038/cjg20141116, 2014.
- Titheridge, J. E.: The slab thickness of the mid-latitude Ionosphere, *Planet Space Sci.*, 21, 1775–1793, 1973.
- Weng, L. B., Fang, H. X., Zhang, Y., Yang, S. G., and Wang, S. C.: Ionospheric TEC, NmF2 and slab thickness over the Athens region, *Chinese Journal Geophysics*, 55, 3558–3567, 2012.
- Yu, T., Wan, W., Liu, L., and Zhao, B.: Global scale annual and semi-annual variations of daytime NmF2 in the high solar activity years, *J. Atmos. Sol.-Terr. Phys.*, 66, 1691–1701, 2004.
- Yue, X., Schreiner, W. S., Lei, J., Sokolovskiy, S. V., Rocken, C., Hunt, D. C., and Kuo, Y.-H.: Error analysis of Abel retrieved electron density profiles from radio occultation measurements, *Ann. Geophys.*, 28, 217–222, doi:10.5194/angeo-28-217-2010, 2010.
- Yue, X., Schreiner, W. S., Kuo, Y. H., and Lei, J.: Ionosphere equatorial ionization anomaly observed by GPS radio occultations during 2006–2014, *J. Atmos. Sol.-Terr. Phys.*, 129, 30–40, 2015.
- Zakharenkova, I., Cherniak, I., Krankowski, A., Shagimuratov, I., and Sieradzki, R.: Using of GPS TEC observations and radio occultation measurements for the ionosphere’s monitoring, *IGS workshop 2012, Olsztyn, Poland*, 23–27 July 2012.